

Comparison of Porous and Direct Volumetric Integration FW-H Formulation for Acoustic Prediction

Yuan Zhuang¹, Luchun Yang², Weiwen Zhao¹, Decheng Wan^{1*}

¹ Computational Marine Hydrodynamic Lab (CMHL), School of Naval Architecture, Ocean and Civil Engineering, Shanghai Jiao Tong University, Shanghai, China

² Wuhan Second Ship Design and Research Institute, Wuhan, China

* Corresponding Author

ABSTRACT

In the present work, two integration methods of FW-H formulation for hydroacoustic prediction are adopted and compared. One of the methods uses porous surface integration method, the other is direct volumetric integration with a dual mesh technique. The numerical model is the flow past a circular cylinder. The setup of simulation case of the two methods keeps the same. The near-field and far-field sound pressure level are compared between these two methods. It is shown that peak value frequency of sound pressure level of both methods is around the shedding frequency of the cylinder. The near-field sound pressure level of those two methods has small differences while the far-field sound pressure levels are large. At last, the efficiency and disk storage of these two methods are also compared. With the dual mesh technique, the volumetric integration method shows small time cost in the simulation.

KEY WORDS: Ffowcs Williams-Hawkings analogy; OpenFOAM; libAcoustics; Dual mesh technique

INTRODUCTION

Nowadays, the sound problem in hydrodynamics became essential. Many numerical methods have been done to solve these kinds of problems. A popular numerical method to predict fluid noise is coupled Computational Fluid Method (CFD) with acoustic analogies. One of the widely used numerical approach to simulate acoustic analogy is the Ffowcs Williams-Hawkings (FW-H) analogy. The contribution of Lighthill stress tensor which is a quadruple source term can be directly calculated with volumetric integration, or it can be calculated on a porous surface.

These two methods both have their own advantages and disadvantages. For example, the porous surface integration method is sensitive to the choice of porous surface as well as the fluid data on the porous surface. Rahier et al (2015) pointed out that a spurious noise would be generated when the turbulent flow crossed through the porous surface. They thought the spurious noise generated due to the lack of volumetric terms. Cianferra et al (2019) compared porous surface integration method with volumetric integration method, and found out that under the low frequency, the accuracy of porous surface integration method is lower

than both volumetric integration and linear Curle method. If only considered far-field noise, the nonlinear term of the sound decreased rapidly.

Therefore, to choose a suitable method to predict the quadruple source term is nonnegligible in hydrodynamic noise. Meanwhile, Cianferra et al (2019) didn't mention the huge storage in computers and large cost in simulation time of volumetric integration method. Wang et al (2022) provided a new method with a dual-mesh technique to solve this problem. The method is carried out with a fine CFD mesh and a relatively coarser acoustic mesh which is used for acoustic calculation. They thought this method can reduce the computational disk storage and simulation time cost.

In this paper, two different solving methodologies are adopted to find out a powerful tool for the noise prediction. The calculations are carried out coupled CFD method for the acoustic assessment. The fluid field simulation chooses Large-Eddy Simulation (LES). The porous FW-H methodology is achieved by an open-source package OpenFOAM implemented the libAcoustics library (Epikhin et al, 2015). The direct FW-H methodology is applied through a dual mesh technique. The sound source information is mapped onto acoustic mesh to reduce the simulation time. A flow past a circular cylinder is considered to be the numerical model. The near-field and far-field acoustic pressures are calculated, as well as calculation time is included to compare the accuracy and efficiency of these two methods.

METHODOLOGY

Ffowcs Williams-Hawkings analogy

The Lighthill analogy (Lighthill, 1954) is derived from Navier-Stokes equation. The FW-H equation (Ffowcs, 1969) is based on the Lighthill equation:

$$\left(\frac{1}{c_0^2} \frac{\partial^2}{\partial t^2} - \nabla^2\right) p' = \frac{\partial}{\partial t} (Q \delta(f)) - \frac{\partial}{\partial x_i} (F_i \delta(f)) + \frac{\partial^2}{\partial x_i \partial x_j} (H(f) T_{ij}) \quad (1)$$

where $Q = (\rho_0 v_i + \rho(u_i - v_i)) \frac{\partial f}{\partial x_i}$, $F_i = (P_{ij} + \rho u_i(u_j - v_j)) \frac{\partial f}{\partial x_i}$,

$T_{ij} = P_{ij} + \rho u_i u_j - c_0^2 \rho' \delta_{ij}$ is the Lighthill stress tensor. $p' = c_0^2(\rho - \rho_0)$ is the derivation from undisturbed fluid, δ_{ij} is the Dirac delta function, $H(f)$ is the Heaviside function:

$$H(f) = \begin{cases} 1, f(x, t) > 0 \\ 0, f(x, t) < 0 \end{cases} \quad (2)$$

P_{ij} is the compressible stress tensor, in the incompressible fluid can be written as:

$$P_{ij} = p \delta_{ij} - \tau_{ij} \quad (3)$$

where p is the local pressure and τ_{ij} is viscous stress tensor. A common integral solution of FW-H equation is Farassat Formulation 1A. The sound pressure at observer \mathbf{x} and time t can be divided into thickness term p_r' and loading term p_L' :

$$4\pi p_r' = \int_{f=0} [\frac{\rho_0(\dot{U}_n + U_n)}{r(1-M_r)^2}]_{ret} dS + \int_{f=0} [\frac{\rho_0 U_n [r \dot{M}_r + c_0(M_r - M^2)]}{r^2(1-M_r)^3}]_{ret} dS \quad (4)$$

$$4\pi p_L' = \frac{1}{c_0} \int_{f=0} [\frac{\dot{L}_r}{r(1-M_r)^2}]_{ret} dS + \int_{f=0} [\frac{L_r - L_M}{r^2(1-M_r)^2}]_{ret} dS + \frac{1}{c_0} \int_{f=0} [\frac{L_r \{r \dot{M}_r + c_0(M_r - M^2)\}}{r(1-M_r)^3}]_{ret} dS \quad (5)$$

where $r = |\mathbf{x} - \mathbf{y}|$ is the length of the radius between source sound and observation point; $M_i = \frac{v_i}{c_0}$ presents the vectorial Mach number.

$$U_i = v_i + \frac{\rho}{\rho_0} (u_i - v_i) \quad (6)$$

$$L_i = p n_i + \rho u_i (u_n - v_n) \quad (7)$$

The volumetric sound source $4\pi p_{vol}' = \frac{\partial^2}{\partial x_i \partial x_j} \int_V [\frac{T_{ij}}{r(1-M_r)}]_{ret} dV$ can be direct calculated through a work from Nyandeni and Chinyoka(2021):

$$4\pi p_{vol}' = \frac{1}{c_0^2} \int_{f>0} [\frac{\hat{r}_i \hat{r}_j \ddot{T}_{ij}}{r}]_{ret} dV + \frac{1}{c_0} \int_{f>0} [\frac{3\hat{r}_i \hat{r}_j - \delta_{ij}}{r^3} (r \dot{T}_{ij} + T_{ij})]_{ret} dV \quad (8)$$

where \hat{r}_i is the unit vector of the direction of r_i .

Or the volumetric sound can be calculated through a control surface, which also can be called 'permeable' or 'porous' surface integration. A quadrupole is being a partial cancellation of two more efficient dipoles(Greschner et al, 2008).

Turbulent model

The turbulent model is chosen to be Large-Eddy Simulation (LES). The vortex of large scale is solved directly through N-S equation (Schmalz, 2015):

$$\frac{\partial \bar{u}_i}{\partial x_i} = 0 \quad (9)$$

$$\frac{\partial \bar{u}_i}{\partial t} + \frac{\partial \bar{u}_i \bar{u}_j}{\partial x_j} = -\frac{1}{\rho_0} \frac{\partial \bar{p}}{\partial x_i} + \nu \frac{\partial^2 \bar{u}_i}{\partial x_j \partial x_j} - \frac{\partial \tau_{ij}^{SGS}}{\partial x_j} \quad (10)$$

where \bar{u}_i represents the fluid velocity component in the x direction with filtering operation, ρ_0 is the fluid density; ν is the kinematic viscosity.

τ_{ij}^{SGS} is the SGS (sub-grid scale Reynolds) stress tensor with $\tau_{ij}^{SGS} = \overline{u_i u_j} - \bar{u}_i \bar{u}_j$. The SGS tensor represents the effect of the large-scale fluctuations on the small-scale vorticity. It can be modeled with Smagorinsky model:

$$\tau_{ij}^{SGS} - \frac{1}{3} \tau_{kk}^{SGS} \delta_{ij} = -2\nu_t \bar{S}_{ij} \quad (11)$$

$$\bar{S}_{ij} = \frac{1}{2} \left(\frac{\partial \bar{u}_j}{\partial x_i} + \frac{\partial \bar{u}_i}{\partial x_j} \right) \quad (12)$$

where ν_t is SGS eddy viscosity:

$$\nu_t = (C_s \Delta)^2 \left| \bar{S}_{ij} \right| = (C_s \Delta)^2 \sqrt{2 \bar{S}_{ij} \bar{S}_{ij}} \quad (13)$$

where C_s is the Smagorinsky constant and Δ is the filter width. In this paper, we applied the LES model is OpenFOAM which implements the Smagorinsky model as $\nu_t = C_k \Delta^2 \sqrt{C_k / C_e} \left| \bar{S}_{ij} \right|$. The default value for the constants is $C_k = 0.094$ and $C_e = 1.048$.

Dual mesh technique

Most acoustic analogy with CFD method adopted post-processing to avoid large time cost in simulations. However, with CFD results contains the sound source information, the large storage of the disk can't be ignored if this conduction applied. Wang et al (2022) provided a dual mesh technique to solve this problem.

Integrals in Eqs. (4), (5) and (8) are calculated in a first order discretized scheme. The sound sources are calculated in CFD mesh while during the simulation, and interpolated in the acoustic mesh. The integration of sound source term is calculated as:

$$\Phi_i^{acoustic} = \sum_{j=0}^{N_i} \varphi_{ij}^{CFD} \cdot V_{ij}^{CFD} \quad (14)$$

where φ is an arbitrary quantity, $\Phi_i^{acoustic} = (\int \varphi dV)_i^{acoustic}$ represents the volumetric integration. The subscript (i, j) is the association between j^{th} CFD cell and i^{th} acoustic mesh cell. V_{ij}^{CFD} is the volume of CFD cell.

NUMERICAL SIMULATION

Numerical Setup

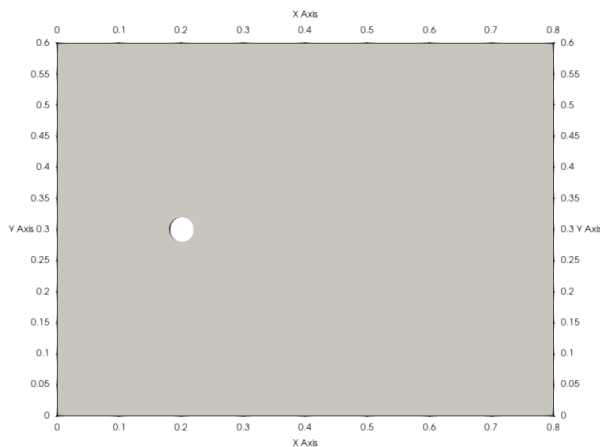
Both fluid and acoustic simulation are based on the open-source OpenFOAM library, solved in Finite Volume Method (FVM). The solver we choose is pimpleFoam with 2nd order upwind scheme for convection term discretization. A 2nd order implicit scheme is applied to discretize time. The porous surface integration method as well as volumetric directly integration is adopted as a library of OpenFOAM.

The numerical model was chosen to be a 2-dimensional circular cylinder with a uniform incompressible flow passing by. The diameter of the circular cylinder is 0.04m with incoming flow velocity of 0.025m/s. The detailed parameters of the circular cylinder and the simulation case are described in table 1.

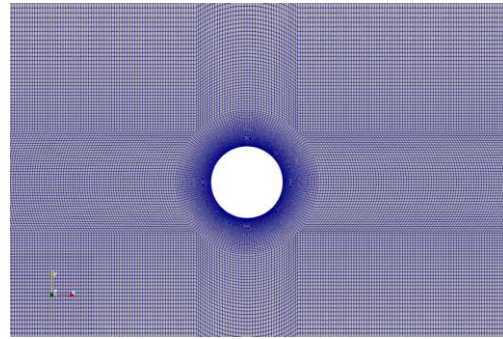
Table 1 Parameters of the circular cylinder

Parameters	Value
Circular diameter (m)	0.04
Flow speed (m/s)	0.025
Kinematic viscosity (m ² /s)	1e-5
Reynolds number	100
Strouhal number	0.159
Shedding frequency (Hz)	0.1

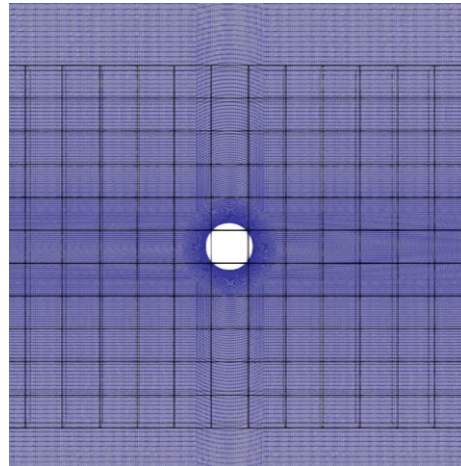
Fig. 1 shows the setup of computational domain and the mesh distribution of the simulation case separately. The inlet is about 5D from the front cylinder. The selected CFD computational domain is described as $0 < x < 0.8m$, $0 < y < 0.6m$. The mesh of the case is generated by *blockMesh*, a mesh generation tool from OpenFOAM. The mesh around the circular cylinder is refined to confirm $y^+ = 1$. The total mesh number is 0.12 million. The acoustic mesh generation is shown in Fig. 1(c). The grid number along the x direction is 26 while along the y direction is 11.



(a) The setup of computational domain



(b) The mesh distribution around the cylinder

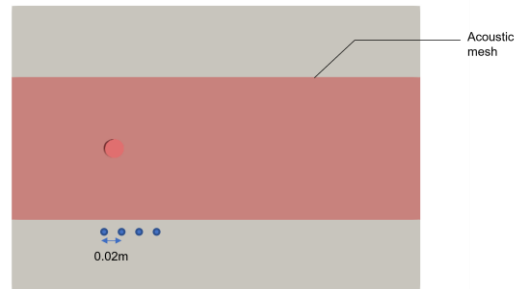


(c) The acoustic mesh generation (black one)

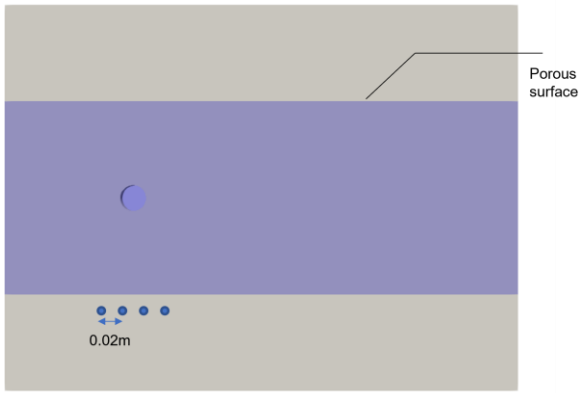
Fig. 1 The background and mesh generation of the simulation case

Two different test cases are shown in Fig.2. Fig. 2(a) illustrates the dual mesh technique case with acoustic mesh distribution. The red domain indicates the setup of the acoustic mesh area. In order to compare these two methods, the same setup of porous surface integration method is shown in Fig.2 (b). The area of both porous surface and acoustic mesh is set as $0 < x < 0.8m$, $0.15m < y < 4.5m$, which includes the wake flow of the circular cylinder. The velocity flow and streamline of the cylinder are shown in Fig. 3 and Fig.4.

Four observation points are set near the area of integration surface and volume in order to study the near field acoustic characteristics, as shown in Fig.2. The space between each probe along x is 0.02m, they are (0.18, 0.13, -0.01), (0.2, 0.13, -0.01), (0.22, 0.13, -0.01) and (0.24, 0.13, -0.01).



(a) The setup of dual mesh technique case



(b) The setup of porous surface integration case

Fig. 2 The pre-process of computational domain

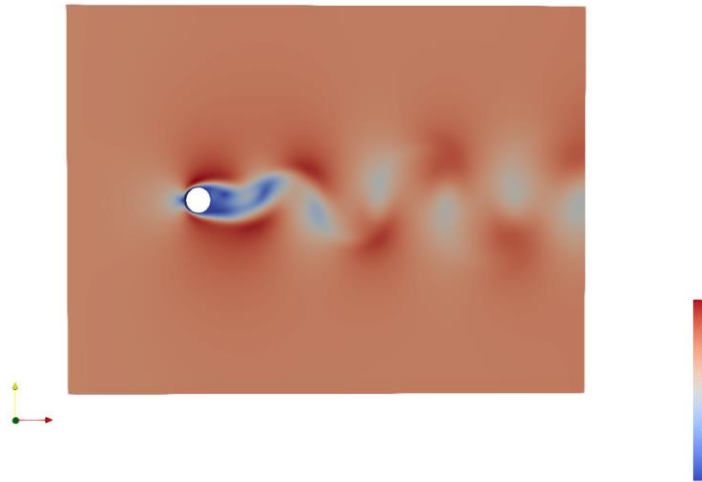
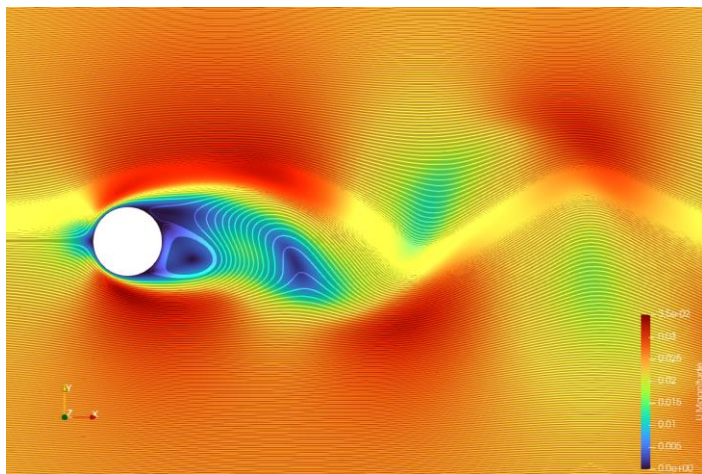
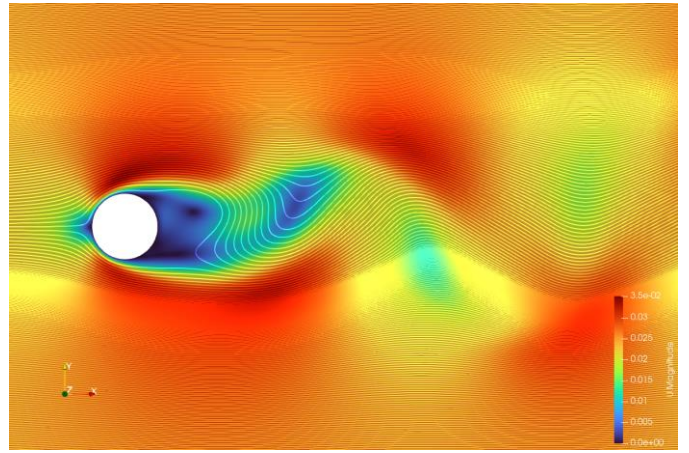


Fig. 3 The wake flow of the circular cylinder



(a) Simulation time= 195s



(b) Simulation time= 200s

Fig. 4 Stream lines in two moments

RESULTS AND DISCUSSION

Hydroacoustic analysis

In order to verify the fidelity of volumetric integration method and porous surface integration method, the pressure spectrum of these two methods is compared with hydrodynamic pressure in LES. The four acoustic probes as well as pressure probes are illustrated in Fig. 4.

We use the formulation of sound pressure level (SPL) to describe the acoustic pressure and the fluid pressure as:

$$SPL = 20 \lg \frac{p'}{p_0} \quad (15)$$

It can be seen that the curve of the pressure spectrum of both these two methods have the peak value. The corresponding frequency of the peak value is the same with that in LES, which is around the shedding frequency. The maximum SPL appears around the shedding frequency, which proves that it will generate the largest noise when under the shedding frequency of the cylinder. The comparison between the peak value frequency and shedding frequency is illustrated in Table 2.

Table 2 The comparison between peak value frequency and shedding frequency

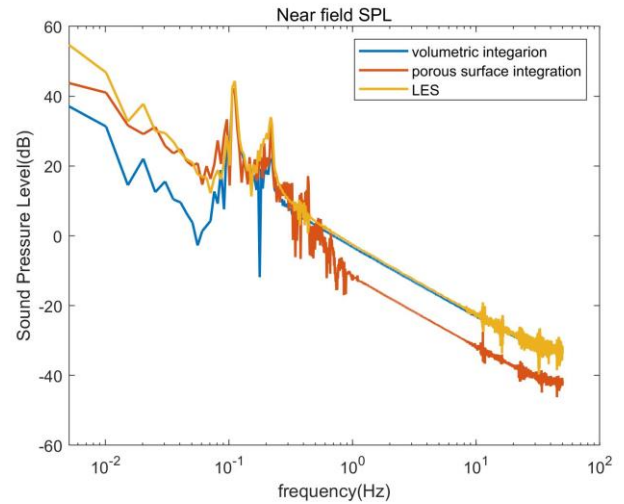
Name	Peak value frequency	Shedding frequency	error
Probe 1	0.106	0.1	10.6%
Probe 2	0.106	0.1	10.6%
Probe 3	0.106	0.1	10.6%
Probe 4	0.106	0.1	10.6%

The comparison of peak value among the two methods and LES is displayed in Table 3. The porous surface integral method and volumetric integral method both has discrepancies in the value when comparing with that of LES. Except probe 1, the errors between volumetric integration method and LES are smaller than that of porous surface integration method. Meanwhile, the peak value of volumetric integration and LES is relatively stable in these four pressure probes, but porous surface method shows a fluctuate value in these four pressure probes.

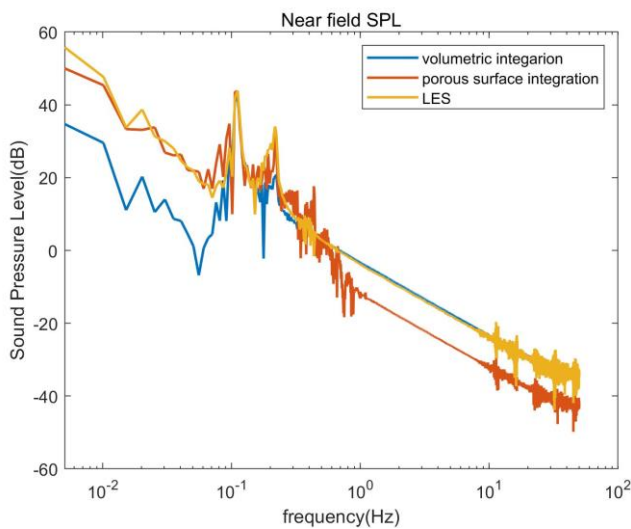
Table 3 Comparison among the forces of present method, experiment and other numerical methods

Name	Porous surface integration	Volumetric integration	LES	Error(L-P)	Error(L-V)
Probe 1	43.69	42.12	43.93	0.55%	4.10%
Probe 2	46.59	41.85	42.82	-8.80%	2.30%
Probe 3	41.75	42.17	44.38	5.90%	4.97%
Probe 4	40.21	42.06	44.52	9.68%	5.52%

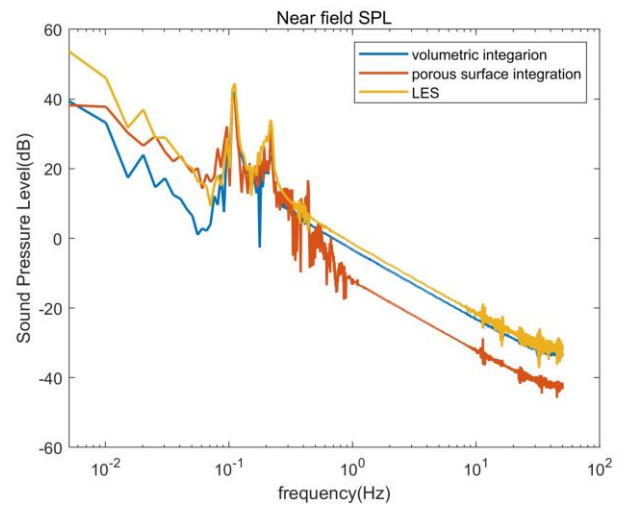
When considering SPL in low frequency and high frequency, which are shown in Fig. 5, the porous surface method has more accurate prediction in low frequencies while volumetric integration method has more accurate prediction in high frequencies.



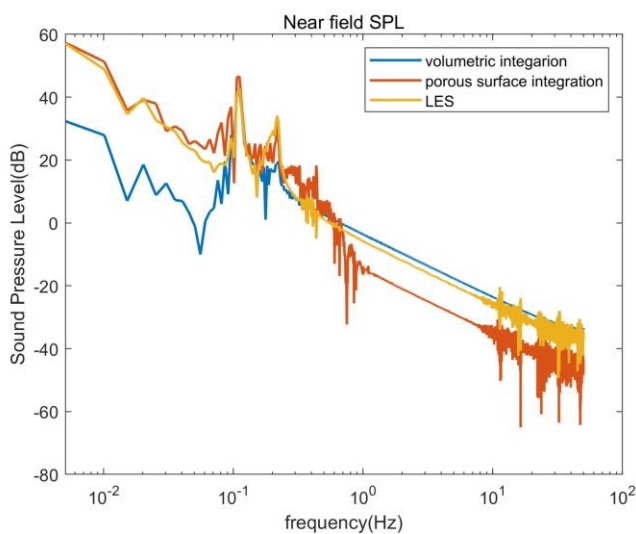
(c) pressure spectrum of probe 3



(a) pressure spectrum of probe 1



(d) pressure spectrum of probe 4



(b) pressure spectrum of probe 2

Fig. 5 The pressure spectrum of four probes with volumetric integration (blue line), porous surface integration (red line) and LES (yellow line).

Far-field SPL

In order to compare the far-field SPL, 8 acoustic pressure probes are set around the cylinder, shown in Fig.6. Those 8 probes are symmetric of the center of the cylinder. The distance from probe 1, 3, 5, 7 to the circular center is 70D, while the distance of probe 2, 4, 6 and 8 is 256D.

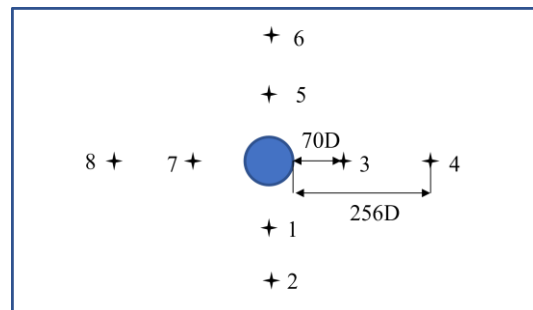
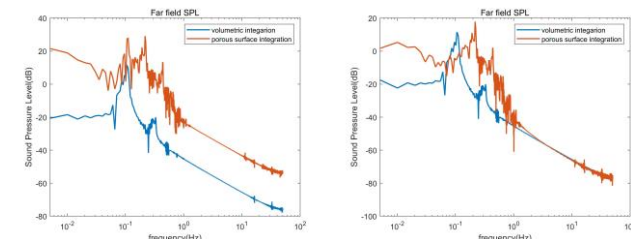


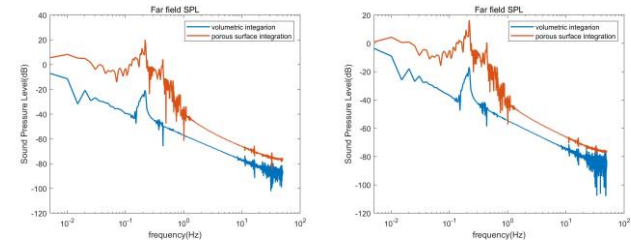
Fig. 6 The setup of acoustic pressure probes

The far-field SPL of porous surface integration method and volumetric integration method is shown in Fig.7. For the sound field generated by the flow over the circular cylinder is symmetric, we put the corresponding probes together. It can be seen that the discrepancies in far-field sound pressure level between these two methods are obvious. The values of far-field sound pressure level in porous surface integration method are all larger than those in volumetric integration method.

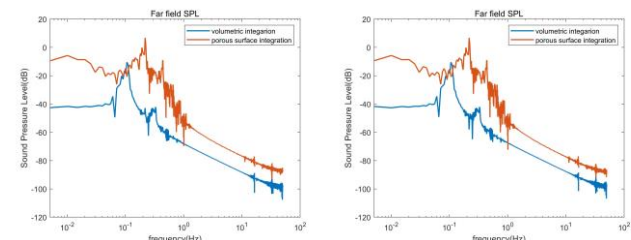
Fig7 (a) and (b) illustrates the probes 1 and 5 which are near the cylinder. The sound field in probe 1 and 5 are the same due to the symmetry of the flow around the cylinder, however, the results of porous surface integration method are asymmetric. The peak value frequency of volumetric method is kept around the shedding frequency, while that of porous surface integration method is derivate from the shedding frequency. The sound field in probe 3 and 7 are almost symmetric in both methods. However, their peak value frequencies are derivate from the shedding frequency.



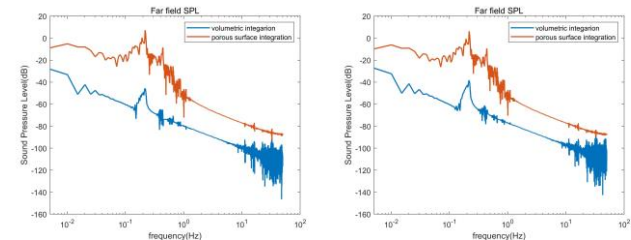
(a) sound pressure level of probe 1 (left) and probe 5 (right)



(b) sound pressure level of probe 3 (left) and probe 7 (right)



(c) sound pressure level of probe 2 (left) and probe 6 (right)



(d) sound pressure level of probe 4 (left) and probe 8 (right)

Fig. 7 The sound pressure level (SPL) of eight probes with volumetric integration (blue line), porous surface integration (red line)

Fig 7 (c) and (d) are the SPL of far probes around the cylinder. The SPL of far probes shows symmetric in those two methods. The peak value frequency of probe 2 and 6 of volumetric integration method is around the shedding frequency, while the rest of them are larger than shedding frequency.

The results are similar with the research which was done by Cianferra et al (2019), they also found that in far-field sound prediction, the porous surface method shows difference with other methods (Eg. Volume direct solution and Curle equation). Meanwhile, we found that the peak value frequency of volumetric integration method in the probes along the horizontal direction are around the shedding frequency, while along the vertical direction of cylinder are larger than shedding frequency. The peak value in horizontal direction is larger than that in vertical direction.

Efficiency and Time Cost

Table.4 lists the CPU time when simulating the case in porous surface integration method and volumetric integration method separately. The simulations were calculated with one core in processor with Intel i7-4790 CPU 3.6GHz×8. Under the same circumstance, the volumetric integration cost less simulation time than that of porous surface integration method. The former method saves 0.99 times of simulation time than that in latter method.

The disk storage of these two methods is also compared in table 4. Both simulation cases include 100 steps of field information. The volumetric integration method has more disk storage than that of porous surface integration method.

Table 4 The comparison of CPU time and Disk storage

Name	Porous surface integration	Volumetric integration	Factor
CPU time (s)	49074.54	48684.82	0.992
Disk storage (MB)	846.29	1023.59	1.21

CONCLUSIONS

This paper compared two popular methods applied in hydroacoustic analysis, which are porous surface integration and volumetric integration methods. The numerical model is a uniform flow pass through a two-dimensional circular cylinder with low Reynolds number. The volumetric integration method applied a dual mesh technique to improve the efficiency of the simulation.

The sound pressure level of near-field and far-field of these two methods are analyzed and compared. In near-field SPL, the results of volumetric integration method are closer to that of LES. The porous surface integration method shows better results in low frequency while the volumetric method shows better results in high frequency. In far-field SPL, the discrepancies between these two methods are obvious. The volumetric method has more reasonable results than that of surface porous method. Comparing the CPU time and disk storage, these two methods have their own advantages. The volumetric integration with dual mesh technique is more efficiency than the surface porous surface integration.

In the future, this paper needs to improve in two ways. On the one hand,

the discussions need to be done to figure out the influence of the acoustic mesh. In the paper of Wang et al (2022), the proper ratio between acoustic mesh and CFD mesh is not provided. In this paper we applied a medium one referring to their research. However, the influence of the ratio between these two meshes needs to be clearer. On the other hand, the LES method is not proper for two-dimensional case. The aim we applied LES method in this paper is due to a subsequent three-dimensional case. We want to eliminate the discrepancies in the choice of turbulence model.

ACKNOWLEDGEMENTS

This work was supported by the National Natural Science Foundation of China (52201372), and the National Key Research and Development Program of China (2019YFB1704200), to which the authors are most grateful.

REFERENCES

- Cianferra M, Ianniello S, Armenio V (2019). "Assessment of methodologies for the solution of the Ffowcs Williams and Hawkings equation using LES of incompressible single-phase flow around a finite-size square cylinder." *Journal of Sound and Vibration*, 453: 1-24.
- Epikhin, A., Evdokimov, I., Kraposhin, M., Kalugin, M., Strijhak, S (2015). "Development of a Dynamic Library for Computational Aeroacoustics Applications Using the OpenFOAM Open Source Package." *Procedia Computer Science*, 66: 150-157.
- Ffowcs Williams JE, Hawkings DL. (1969) "Sound generated by turbulence and surfaces in arbitrary motion." *Phil Trans Roy Soc A*. 264(1151):321-42
- Greschner, B., Thiele, F., Jacob, M. C., & Casalino, D. (2008). "Prediction of sound generated by a rod-airfoil configuration using EASM DES and the generalised Lighthill/FW-H analogy." *Computers & fluids*, 37(4), 402-413.
- Lighthill, M. J. (1952). "On sound generated aerodynamically I. General theory." *Proceedings of the Royal Society of London. Series A. Mathematical and Physical Sciences*, 211(1107), 564-587.
- Nyandeni, Z., Chinyoka, T (2021). "Computational aeroacoustic modeling using hybrid Reynolds averaged Navier-Stokes/large-eddy simulations methods with modified acoustic analogies." *Internat. J. Numer. Methods Fluids*.
- Rahier G, Huet M, Prieur J (2015). "Additional terms for the use of Ffowcs Williams and Hawkings surface integrals in turbulent flows." *Computers & Fluids*, 120: 158-172.
- Schmalz, J., Kowalczyk, W (2015). "Implementation of acoustic analogies in OpenFOAM for computation of sound fields." *Open Journal of Acoustics*, 5(02), 29.
- Wang Y, Mikkola T, Hirdaris S (2022). "A fast and storage-saving method for direct volumetric integration of FWH acoustic analogy." *Ocean Engineering*, 261: 112087.